Structural and Lattice Dynamical Investigation of Models for Reactions in Organic Crystals

John J. Stezowski,* Nathaniel M. Peachey, Peter Goebel, and Craig J. Eckhardt*

Contribution from the Department of Chemistry, University of Nebraska-Lincoln, Lincoln, Nebraska 68588-0304

Received January 22, 1993

Abstract: The topochemical postulate and phonon assistance are two models used for understanding solid-state reactions. Neither has been studied in a fashion that directly relates the two. This research reports a concerted X-ray crystallographic and polarized, single-crystal Raman scattering study which investigates the models' applicability in a partially reacted crystal of 2,5-distyrylpyrazine, a prototypical reacting organic solid. The structural results of a partially reacted monomer crystal are related to the change in lattice dynamics observed by Raman scattering for the same system. By use of lattice dynamical calculations, the assignment of modes, and the structure of the partially reacted crystal, a detailed picture of the lattice motions and related displacements involved in the reaction is constructed and related to the topochemical postulate and the mechanism of phonon assistance.

I. Introduction

Solid-state reactions have been the focus of considerable research in recent decades. Almost all work highlights the structural and geometric requirements in determining reactivity. Schmidt and his co-workers first formulated the topochemical postulate which states that a solid-state reaction proceeds with minimum movement of the atoms or molecular groups involved.[1,2] This concept was later generalized to include the idea of minimal distortion of the "reaction cavity" which became necessary to account for the role of hydrogen bonding and other constraints on the solid-state reaction.[3] All of this suggests that the progress of the reaction is controlled by relatively fixed distances and orientation.

The topochemical postulate has been used successfully to determine which molecular crystals will be photoreactive and which will be photostable. This is particularly true for the cinnamic acids and the diacetylenes which have been archetypical solid-state reactions. With few exceptions,[4,5] current evidence for the topochemical postulate is structural and rests on comparison of the separate crystal structures of the reactant and the product with subsequent inference of the most probable pathway between them.

The success of the topochemical postulate in determining reactivity has led a generation of solid-state scientists to focus primarily upon crystal structure in explaining these reactions. However, more thorough substantiation of this postulate requires study of the structural *and* dynamic changes of the lattice throughout the course of the reaction such that the developing product may be observed in the reactant lattice. This must be joined with studies that show dynamical aspects of the reaction through identification of motions of molecules in the unit cell that are involved with the reaction. Such investigation requires related spectroscopic and crystallographic experiments. This paper reports the findings of such a study.

The solid-state structure is ultimately a result of a particular force field generated by the interaction of van der Waals forces within the lattice and thus is itself a derivative of the crystal energetics and lattice dynamics. The mechanism of "phonon assistance" has been suggested as a more dynamical explanation for these reactions.[6] By this mechanism, the collective molecular vibrations, phonons, may promote product formation analogous to the role of collisions in gas-phase reactions. Clearly, only phonons with motions along the reaction coordinates that bring the reacting molecules into a favorable position to form the product could "assist" the reaction. Such phonons are posited to shift to lower frequency with increased formation of developing product. This decrease in phonon frequency, termed mode softening in analogy to similar behavior in phase transitions, is accompanied by an increased amplitude of the vibrational oscillations which further promote the interactions of the reactants.

For phonon assistance to be consistent with the topochemical postulate, only certain lattice phonons or lattice modes should participate in phonon assistance. Those phonons that are intimately involved in the reaction mechanism are expected to have displacements that introduce the least motion possible in order for the reaction to occur. This should be true of the topochemical postulate in its later form since the reaction cavity may be viewed as defined by the full complex motion of the lattice modes, which rarely will have sole motions along the path of the reaction coordinate. Thus, the reaction cavity also requires restricted if not minimal motion. If this is not the case, the topochemical postulate is violated. Indeed, in order to both the topochemical postulate and phonon assistance to correctly rationalize a particular solid-state-reaction mechanism, each must be consistent with the other.

Thus a more comprehensive understanding of solid-state reactions is gained when structural changes during the course of the reaction are correlated with quantitative information on energetics derived from vibrational spectroscopy and lattice dynamical studies. Phonons, like intramolecular vibrations, are vibrations that result from a particular potential energy surface. In a solid-state reaction, the crystal potential energy surface is modified as the solid undergoes the chemical transformation. Consequently, the phonons will also be affected by this transformation. These changes can be conveniently monitored with various vibrational spectroscopies such as Raman scattering. In investigating solid-state-reaction dynamics both the topochemical

* Authors to whom correspondence should be addressed.

(1) Cohen, M. D.; Schmidt, G. M. J.; Sonntag, F. I. *J. Chem. Soc.* **1964**, 2000. Schmidt, G. M. J. *J. Chem. Soc.* **1964**, 2014. Bregman, J.; Schmidt, G. M. J. *J. Am. Chem. Soc.* **1962**, *84*, 3785. Sadeh, T.; Schmidt, G. M. J. *J. Am. Chem. Soc.* **1962**, *84*, 3970.

(2) Schmidt, G. M. J. *Photoreactivity of the Photoexcited Organic Molecule*; Interscience: New York, 1967.

(3) Cohen, M. D. *Angew. Chem., Int. Ed. Engl.* **1975**, *14*, 386.

(4) Pfluger, C. E.; Ostrander, R. L. *Photochem. Photobiol.* **1989**, *49*, 375.

(5) McBride, J. M.; Segmuller, B. E.; Hollingsworth, M. D.; Mills, D. E.; Weber, B. A. *Science* **1986**, *234*, 830.

(6) Prasad, P. N. In *Organic Solid State Chemistry*; Desiraju, G., Ed.; Elsevier: Amsterdam, 1987; Vol. 32, Studies in Organic Chemistry, p 117. Prasad, P. N.; Swiatkiewicz, J.; Eisenhardt, G. *Appl. Spectrosc. Rev.* **1982**, *18*, 59. Prasad, P. N., *Stud. Org. Chem.* (*Amsterdam*) **1987**, *32*, 117.

0002-7863/93/1515-6499$04.00/0

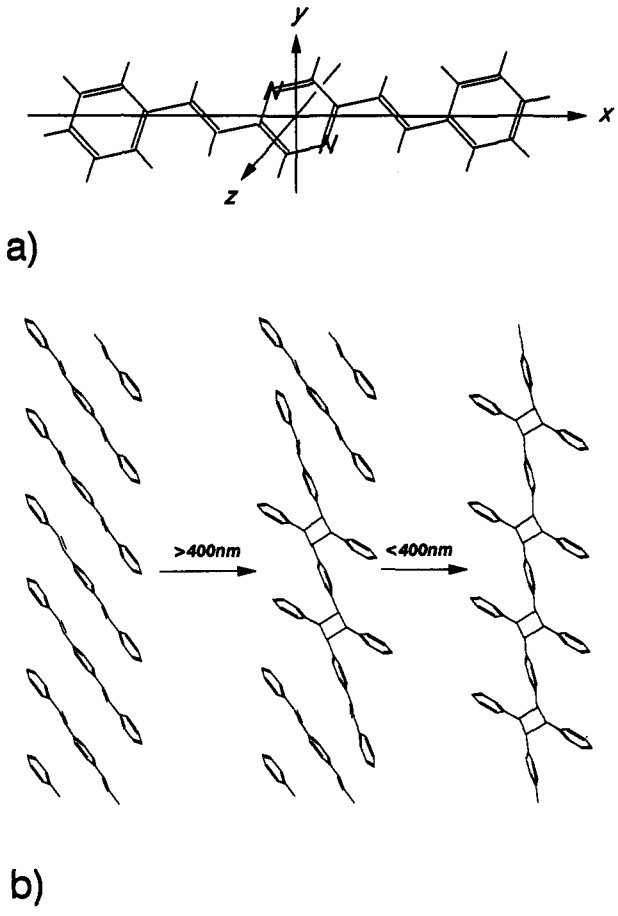

Figure 1. (a) The DSP molecule with axial assignments. (b) The reaction of DSP showing formation of the oligomer and polymer.

postulate and phonon assistance should be revealed by relative displacements of reactant and product molecules. These changes in geometry should be related to normal lattice mode motions that display frequency shifts to lower energy. Since Raman spectroscopy cannot directly yield information about the motions associated with each vibrational mode, lattice dynamical calculations must be used to establish these. Alternatively, in structures where anisotropic displacement parameters (ADPs) can be reliably determined, further correspondence between the structural and spectroscopic results are possible. In such cases, the ADPs should display an elongation in the direction of the vibrational motion of the phonon-assisting modes.

To investigate directly the structural and physical aspects of a solid-state reaction, the 2,5-distyrylpyrazine (DSP) polymerization has been studied by X-ray crystallography and single-crystal Raman spectroscopy. This crystal-to-crystal reaction is an archetypical four-center photochemical cyclomerization where two carbon–carbon double bonds in adjacent molecules form a cyclobutane ring (Figure 1).[7] This reaction proceeds in a two-stage manner. Irradiation with light of wavelength between 480 and 400 nm[8] yields an oligomer which is on the average a trimer. Further or initial irradiation with light of wavelength less than 400 nm causes formation of a high polymer. Recent single-crystal spectroscopy has shown this wavelength dependence of the reaction is due to two separate electronic states.[9,10]

This investigation blends a structural study of a partially reacted DSP crystal using X-ray diffraction with studies of the vibrational Raman spectroscopy and lattice dynamical calculations of a crystal

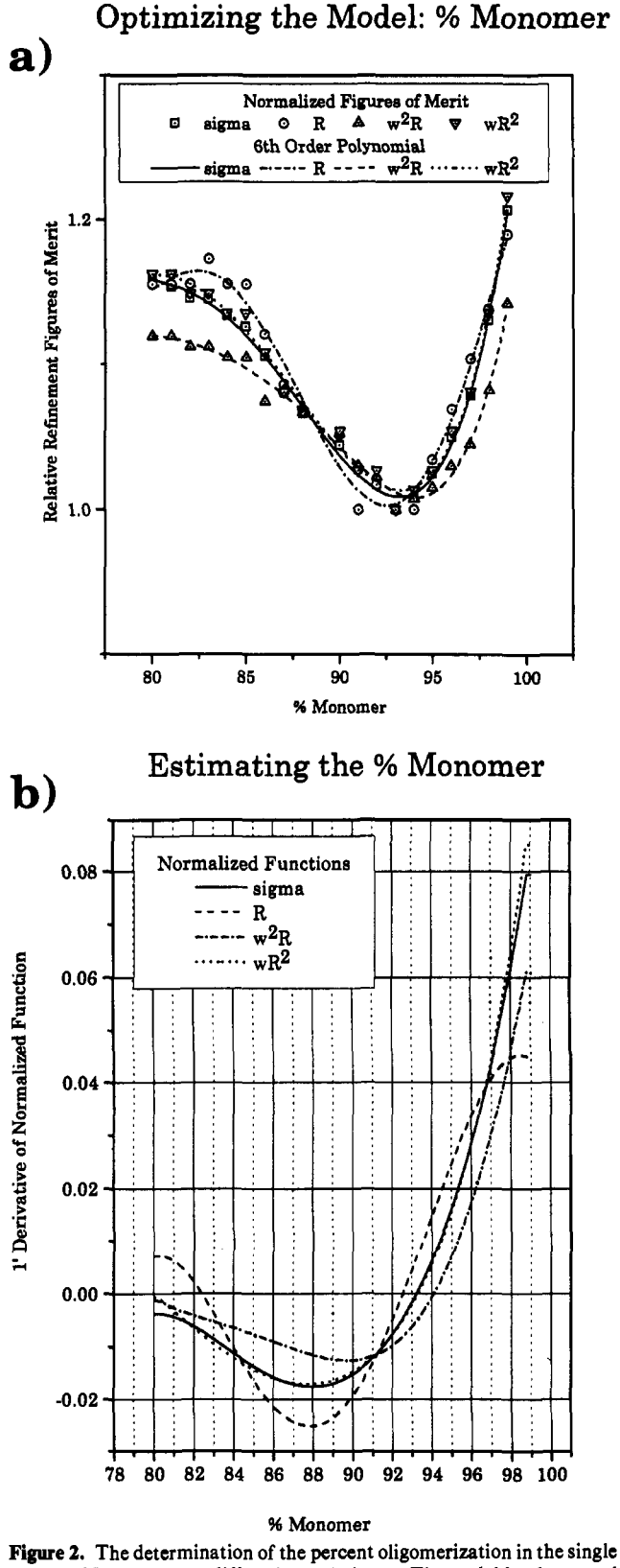

Figure 2. The determination of the percent oligomerization in the single crystal of DSP by X-ray diffraction techniques. The model for the crystal structure was refined in 1% intervals allowing free refinement of both the monomer (anisotropic ADPs) and the oligomer (isotropic ADPs). (a) Normalized conventional crystallographic figures of merit are plotted vs the percent monomer and (b) the first derivative of the curves in plot a are plotted vs percent monomer. The resultant percent monomer at which the first derivative is zero is 93.3(7)%.

that has been taken, within estimated error, to the same degree of reaction as the diffraction experiment. The experimental procedures of the DSP synthesis, crystal growth, and oligomer-

(7) Hasegawa, M.; Suzuki, Y.; Nakanishi, H.; Nakanishi, F. *Prog. Polym. Sci. Jpn.* **1973**, *5*, 143. Wegner, G. *Makromol. Chem. Suppl.* **1984**, *6*, 347.
(8) Braun, H.-G.; Wegner, G. *Mol. Cryst. Liq. Cryst.* **1983**, *96*, 121.
(9) Peachey, N. M.; Eckhardt, C. J. *Chem. Phys. Lett.* **1992**, *88*, 462.
(10) Peachey, N. M.; Eckhardt, C. J. *J. Am. Chem. Soc.* **1993**, *115*, 3519.

Table I. Atomic Positional, Isotropic Displacement,[a] and Site Occupancy Parameters

	x/a	*y/b*	*z/c*	*U*	PP
	(a) The 2,5-Distyrylpyrazine Molecule				
N(1)	0.6068(3)	0.1244(4)	0.5102(1)	0.0677(9)*	0.9300
C(2)	0.4789(3)	0.1443(3)	0.5364(1)	0.060(1)*	0.9300
C(3)	0.6236(3)	−0.0195(4)	0.4751(1)	0.062(1)*	0.9300
C(4)	0.4481(3)	0.2982(3)	0.5766(1)	0.0602(9)*	0.9300
C(5)	0.5330(3)	0.4343(4)	0.5851(1)	0.0595(9)*	0.9300
C(6)	0.5068(3)	0.5907(4)	0.6250(1)	0.0592(9)*	0.9300
C(7)	0.3887(3)	0.6106(4)	0.6633(1)	0.065(1)*	0.9300
C(8)	0.3685(3)	0.7559(5)	0.7016(2)	0.071(1)*	0.9300
C(9)	0.4687(4)	0.8877(4)	0.7020(2)	0.077(1)*	0.9300
C(10)	0.5858(3)	0.8724(4)	0.6645(2)	0.075(1)*	0.9300
C(11)	0.6054(4)	0.7245(4)	0.6261(1)	0.066(1)*	0.9300
H(3)	0.720(2)	−0.043(3)	0.4569(8)	0.058(7)	0.930
H(4)	0.354(2)	0.294(3)	0.5983(9)	0.072(8)	0.930
H(5)	0.628(2)	0.435(3)	0.562(1)	0.078(8)	0.930
H(7)	0.315(2)	0.522(3)	0.6656(9)	0.065(8)	0.930
H(8)	0.279(2)	0.761(3)	0.729(1)	0.094(9)	0.930
H(9)	0.450(2)	0.979(3)	0.731(1)	0.09(1)	0.930
H(10)	0.666(2)	0.968(3)	0.667(1)	0.11(1)	0.930
H(11)	0.693(2)	0.712(3)	0.601(1)	0.080(9)	0.930
	(b) The Oligomer				
N(12)	0.598(8)	0.110(5)	0.514(1)	0.038(3)	0.0700
C(22)	0.471(7)	0.177(3)	0.513(1)	0.038(3)	0.0700
C(32)	0.357(9)	0.063(4)	0.508(2)	0.038(3)	0.0700
C(42)	0.449(4)	0.378(3)	0.5182(7)	0.038(3)	0.0700
C(52)	0.554(2)	0.502(3)	0.5521(7)	0.038(3)	0.0700
C(62)	0.514(2)	0.598(2)	0.6173(7)	0.038(3)	0.0700
C(72)	0.385(2)	0.579(4)	0.6479(7)	0.038(3)	0.0700
C(82)	0.342(5)	0.698(5)	0.6949(9)	0.038(3)	0.0700
C(92)	0.427(7)	0.837(4)	0.713(1)	0.038(3)	0.0700
C(102)	0.557(7)	0.855(3)	0.685(1)	0.038(3)	0.0700
C(112)	0.601(5)	0.735(4)	0.638(1)	0.038(3)	0.0700
H(32)	0.253(8)	0.114(7)	0.502(2)	0.038(3)	0.070
H(42)	0.345(3)	0.397(4)	0.5392(9)	0.038(3)	0.070
H(52)	0.654(2)	0.433(6)	0.5584(9)	0.038(3)	0.070
H(72)	0.312(2)	0.480(5)	0.6335(9)	0.038(3)	0.070
H(82)	0.240(5)	0.686(8)	0.716(1)	0.038(3)	0.070
H(92)	0.39(1)	0.933(5)	0.748(1)	0.038(3)	0.070
H(102)	0.621(9)	0.965(5)	0.698(2)	0.038(3)	0.070
H(112)	0.699(5)	0.757(7)	0.614(1)	0.038(3)	0.070

[a] Displacement parameters marked with an asterisk were refined anisotropically.

ization are described in Section II. The results of the X-ray diffraction are presented in Section III. This is followed by the results from the single-crystal, polarized Raman spectroscopy and the lattice dynamical calculations. In section IV, these results will be combined to present a unified explanation of the motions of the reactant molecules and structural changes resulting from the solid-state reaction of DSP.

II. Experimental Section

DSP was synthesized, extensively purified, and crystallized by slow evaporation from a saturated tetrahydrofuran solution. The molecules pack with orthorhombic *Pbca* space group symmetry with four in the unit cell.[11] Crystals used for the Raman spectroscopy were typically 1 × 1 × 0.75 mm^3. Partially oligomerized crystals were obtained by irradiation of monomer crystals with monochromatized light (490 nm) from a 1000-W quartz halogen lamp. Crystals were continuously rotated perpendicular to the *a* crystallographic axis to compensate for anisotropies arising from crystal optics, polarization effects due to the monochromator, and inhomogeneities in the light source. The extent of oligomerization was determined by dissolving a crystal in a 3-nitrobenzyl alcohol matrix and analyzing fast atom bombardment mass spectrometry data with monomeric DSP as the standard. From the mass spectrum, the percent of oligomerization was calculated as the percent of unreacted monomer remaining in the lattice. In the X-ray diffraction study, the occupancy factor of the oligomer (1,4-cycloaddition product) was determined as part of the crystal structure refinement process. It must be noted that since two monomers react to yield one cyclobutane functionality, the crystallographic occupancy factor is half the value calculated for the percent of oligomerization from mass spectrometry.

The single-crystal, polarized Raman spectra of the DSP crystals were obtained with use of a helium–neon laser as the excitation source. The light passed through a polarizer/rotator and was then focused on the crystal. The scattered beam passed through a collection lens and then the desired polarization was selected before being focused on the monochromator slits. A double-grating 1400 Spex monochromator was used to analyze the scattered radiation. The naturally occurring (100) and (010) faces of the DSP crystal were conveniently used to obtain all the Raman active modes of the D_{2h} factor group. Since the DSP crystal possesses a center of inversion, only those modes associated with librations will be Raman active.

X-ray diffraction data were collected from a partially oligomerized crystal of DSP measuring 0.5 × 0.5 × 0.7 mm^3. The space group was confirmed to be *Pbca* with lattice parameters a = 9.700(3) Å, b = 7.592(2) Å, and c = 20.573(4) Å. With 4 molecules per unit cell, the calculated crystal density is 1.246 g·cm^{-3}. Diffraction intensities were measured at room temperature with a Siemens P3F diffractometer (monochromatized Mo Kα radiation, λ = 0.71069 Å) operating in an ω-scan mode to resolution

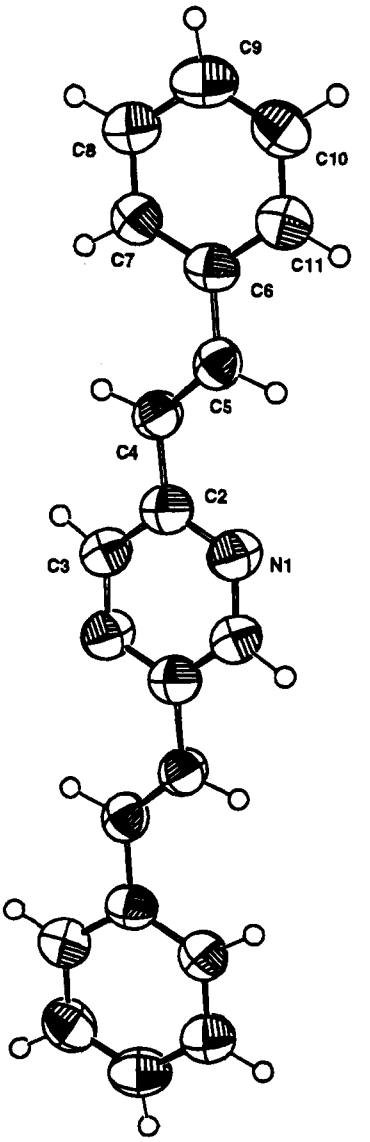

2,5-distyrylpyrazine

Figure 3. The DSP molecule from the crystal structure determination. Atoms are presented with ellipsoids representing the 50% probability level for the anisotropic atomic displacement parameters (ADPs). The molecule has crystallographic inversion symmetry with the operator at the center of the pyrazine ring.

(11) Sasada, Y.; Shimanouchi, H.; Nakanishi, H.; Hasegawa, M. *Bull. Chem. Soc. Jpn.* **1971**, *44*, 1262.

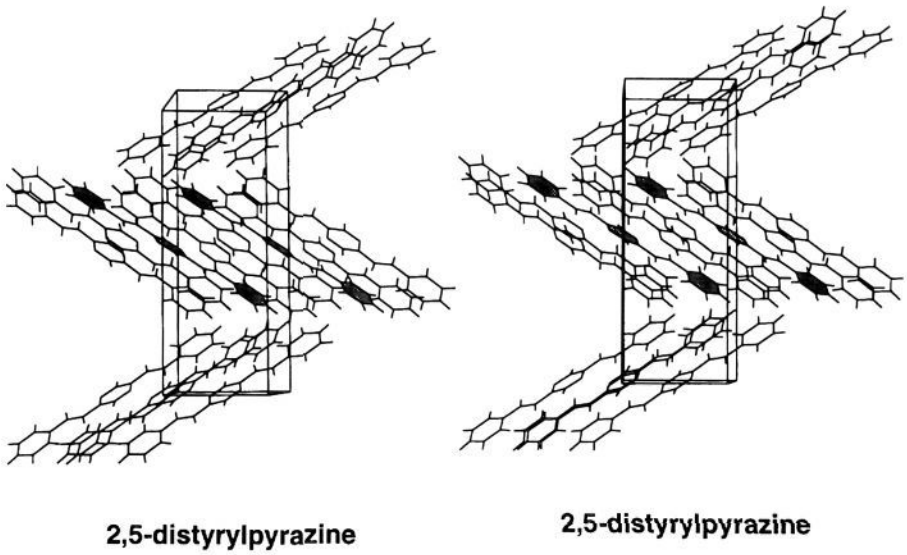

Figure 4. A stereoscopic packing diagram projected onto the *bc* plane of the unit cell. The DSP molecules that are depicted with the shaded rings correspond to those in Figure 5 on which models are superimposed on the electron density contours.

$2\theta_{max} = 55°$ (scan range 1.0°, scan speed ranged from 2.0 to 29.0°/min, background intensities were measured on each side of the reflections ($\Delta\omega$ = 1.0°)); data were corrected for Lorentz and polarization effects.

The initial structural model was determined by direct methods,[12] which revealed atomic positions for all C and N atoms of the DSP molecule. The structural model was further developed by conventional least-squares, Fourier, and difference Fourier techniques. Positions for all hydrogen atoms of the DSP molecule were derived easily from difference Fourier maps. At this stage of model development, two additional peaks of comparable electron density to the hydrogen atoms remained in the asymmetric unit. A model for a trimer of the 1,4-cycloaddition product was constructed by using the molecular modeling program InsightII.[13] By using InsightII to display a difference electron density contour map, the model for the trimer was positioned and oriented, and its conformation was adjusted to fit the residual electron density. Bond distances and angles were not varied from the standard values used to construct the model. The occupancy factor for the oligomer (7 ± 1%) was determined crystallographically by refining the structural model as a function of percent monomer and examining the quality of the converged model to select the best fit (Figure 2). The crystallographic result is consistent with a crystal in which 14 ± 2% of the monomers have undergone a single 1,4-cycloaddition reaction. The least-squares refinement was carried out by refining with ΔF (R_{min} = 12.9%) and with ΔF^2 by three techniques: (a) free refinement of all atomic coordinates, DSP C and N atoms with anisotropic atomic displacement parameters (ADPs) and all others isotropic (R_{min} = 5.2%), (b) DSP treated as in refinement and the oligomer treated as a rigid body with isotropic ADPs (R_{min} = 6.5%), and (c) as in refinement b except that the two symmetry-independent C atoms of the cyclobutane were removed from the rigid body and refined with anisotropic ADPs (R_{min} = 6.4%).

III. Results

A. X-ray Crystallography. Refinement b in which the usual parameters for the monomer were refined and the oligomer was treated as a rigid body with a common isotropic ADP was found to be the most appropriate approach. In refinement a, a number of atoms of the oligomer refined to non-positive definite ADPs, as did one of the two cyclobutane carbon atoms in method c. In refinement b, the refinement was well behaved and converged such that the average shift/error was 0.0006 and the maximum shift/error was 0.0099; the maximum residual electron density was 0.3 e^- Å^{-3}. A total of 1750 reflections contributed to the refinement of 139 parameters to give R = 0.065, R_w = 0.080 ($1/\sigma^2$ weights), and a goodness of fit parameter of 1.77.

The resultant fractional atomic coordinates and isotropic ADPs[14] are contained in Table I. The DSP molecule is illustrated with ellipsoids consistent with the anisotropic ADPs and atom labels in Figure 3; as illustrated, the ellipsoids do not show any particularly large deviations from spherical geometry. Crystal packing is presented in stereoscopic projection in Figure 4; the electron density and difference electron density of the refined model are presented in Figure 5. Examination of Figure 5 demonstrates that the presence of the oligomer at 7 ± 1% occupancy (Figure 2) is clearly revealed by the experimental electron density. The resolution of equivalent atomic positions of the monomer and oligomer in the asymmetric unit is presented in Table II. Numerous sites of analogous atoms in the two components are much closer than the resolution of the data set (0.77 Å), which explains the observation that rigid body refinement for the oligomer atoms gave the best results. The bonding geometry of the DSP molecule, Table III, agrees very well with expectation; the estimated standard deviations in bond distances and angles are typical for a structure derived with a data set of this resolution.

B. Raman Spectroscopy. By observation of the lattice phonons through the course of the reaction using polarized Raman spectroscopy, the evolution of the crystal dynamics can be monitored. Phonons displaying the greatest frequency shifts are expected to have associated molecular motions most involved with the reaction.[6] The ambient temperature, polarized Raman scattering spectra from an unreacted monomer, as well as those from 17 ± 3% oligomerized single crystals, were obtained in configurations for both the A_g and B_g modes.[15] The observed frequencies of the Raman active lattice modes along with the observed shifts of the partially reacted crystal with respect to the original monomer frequencies are shown in Table IV. A B_{2g} mode at 84.25 cm^{-1} displays the largest shift by 2.25 cm^{-1} to lower energy. This mode is likely, therefore, to be involved with the solid-state reaction. The 67.25-cm^{-1} A_g mode and the 136.75-cm^{-1} B_{1g} mode show 1.00-cm^{-1} shifts. These modes are, of course, of interest for any interpretation of this reaction as being mediated by phonon assistance.

C. Lattice Dynamical Calculations. Polarized Raman spectroscopy determines the symmetry of the observed phonon modes,

(12) Hall, S. R.; Stewart, J. M. Xtal3.0, 1990. Unless otherwise indicated this program library was used for crystal structure determination and analysis.

(13) InsightII is available from BioSym Technologies, San Diego, CA.

(14) Anisotropic atomic displacement parameters and a list of structure factors have been deposited in supplementary material.

(15) A complete polarized, single-crystal, Raman study of the DSP monomer and mixed crystals will appear: Peachey, N. M., Eckhardt, C. J. *J. Am. Chem. Soc.*, submitted for publication.

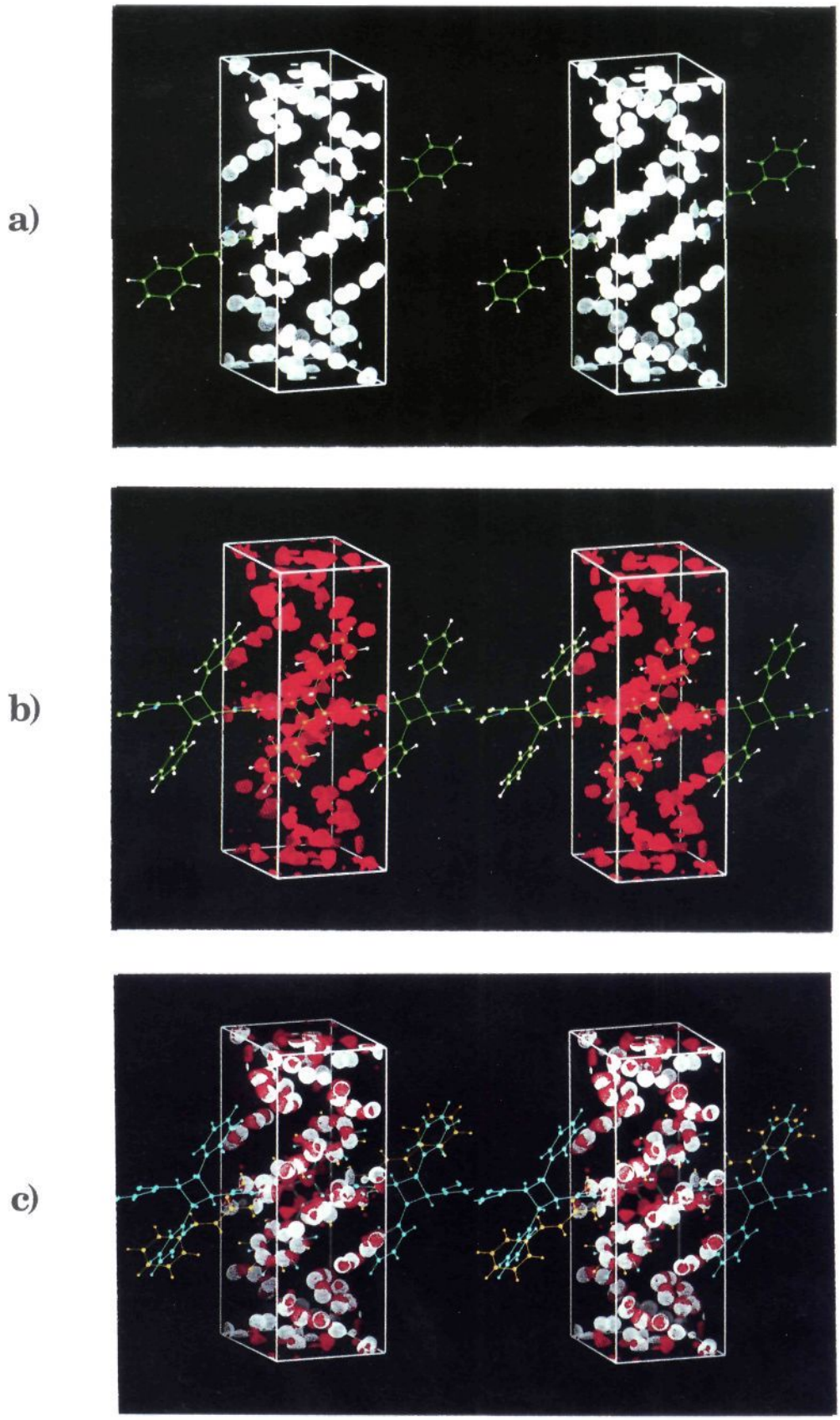

Figure 5. Electron density and difference electron density plots for the 7% oligomerized 2,5-distyrylpyrazine (DSP) crystal. (a) An electron density map for the crystal contoured at 1 e^- Å^{-3}. Stick models for two adjacent DSP molecules are superimposed on the electron density. (b) A difference electron density map, contoured at 0.2 e^- Å^{-3}, in which contributions from the monomer have been removed. In addition to the original DSP pair, a ball and stick model for the oligomer has been superimposed on the map. (c) A plot combining the components of parts a and b to illustrate the effect of repositioning of atoms upon photooligomerization on the electron density in the unit cell.

Table II. Magnitudes of Displacement Atoms of the Oligomer with Respect to Atoms of 2,5-Distyrylpyrazine

	distances (Å)		
N1–N12	0.16(5)	C7–C72	0.40(2)
C2–C22	0.55(2)	C8–C82	0.53(4)
C3–C32	0.52(4)	C9–C92	0.60(5)
C4–C42	1.35(2)	C10–C102	0.52(4)
C5–C52	0.87(2)	C11–C112	0.26(3)
C6–C62	0.18(2)		

Table III. Bonding Geometry in the 2,5-Distyrylpyrazine Molecule[a]

	Bond Distances (Å)		
N1–C2	1.361(4)	C9–C10	1.378(5)
N1–C3	1.320(4)	C10–C11	1.386(5)
C2–C4	1.462(4)	C3–H3	1.03(2)
C2–C3	1.394(4)	C4–H4	1.02(2)
C4–C5	1.333(4)	C5–H5	1.04(2)
C5–C6	1.467(4)	C7–H7	0.98(2)
C6–C7	1.398(4)	C8–H8	1.03(2)
C6–C11	1.395(5)	C9–H9	0.93(2)
C7–C8	1.371(5)	C10–H10	1.07(2)
C8–C9	1.395(5)	C11–H11	1.00(2)
	Bond Angles (deg)		
C2–N1–C3	114.9(3)	N1–C3–H3	117(1)
N1–C2–C4	119.9(3)	H3–C3–C2	118(1)
N1–C2–C3	120.5(2)	C2–C4–H4	114(1)
C4–C2–C3	119.6(3)	C5–C4–H4	121(1)
N1–C3–C2	124.6(3)	C4–C5–H5	119(1)
C2–C4–C5	124.6(3)	C6–C5–H5	114(1)
C4–C5–C6	126.4(3)	C6–C7–H7	123(1)
C5–C6–C7	123.0(3)	C8–C7–H7	115(1)
C5–C6–C11	118.6(3)	C7–C8–H8	118(1)
C7–C6–C11	118.4(3)	C9–C8–H8	124(1)
C6–C7–C8	121.8(3)	C8–C9–H9	114(1)
C7–C8–C9	118.8(3)	C10–C9–H9	126(1)
C8–C9–C10	120.7(3)	C9–C10–H10	121(1)
C9–C10–C11	120.0(3)	C11–C10–H10	118(1)
C6–C11–C10	120.3(3)	C6–C11–H11	121(1)
		C10–C11–H11	119(1)

[a] Estimated standard deviations are in parentheses. bonding geometry for the oligomer model has been deposited as supplementary material.

Table IV. Experimental and Calculated Values of Lattice Phonon Mode Frequencies for Monomer Crystal and Frequency Shifts from the Monomer Values upon Partial Reaction

mode symmetry	monomer mode freq (cm^{-1}) exptl	calcd	mode shift[a] (cm^{-1})
A_g	47.00	46.516	0.00
	67.25	66.505	−1.00
	90.25	100.529	0.00
B_{1g}	38.50	39.075	0.00
	96.50	101.402	0.00
	136.75	143.765	−1.00
B_{2g}	40.75	50.453	0.00
	54.50	57.339	−0.75
	84.25	77.066	−2.25
B_{3g}	29.50	22.434	−0.50
	91.00	90.676	0.00
	137.75	134.851	−0.50

[a] Mode shifts are those observed in the 17% oligomerized crystal with respect to the unreacted monomer crystal.

but it cannot directly reveal the actual motions of the molecules. This requires the use of lattice dynamical calculations which are typically performed with use of the atom–atom potential method.[16]

The minimum potential energy crystal structure for the monomer lattice is first calculated by using a gradient minimization and a Buckingham potential utilizing "universal" parameters.[17] The resulting lattice potential is then used to calculate

(16) White, K. M.; Eckhardt, C. J. *J. Chem. Phys.* **1989**, *90*, 4709; **1990**, *92*, 2214. Kulver, R.; Eckhardt, C. J. *Phys. Rev. B* **1988**, *37*, 5351.

(17) Pertsin, A. J.; Kitaigorodsky, A. I. *The Atom–Atom Potential Method*; Springer-Verlag: Berlin, 1986; p 89.

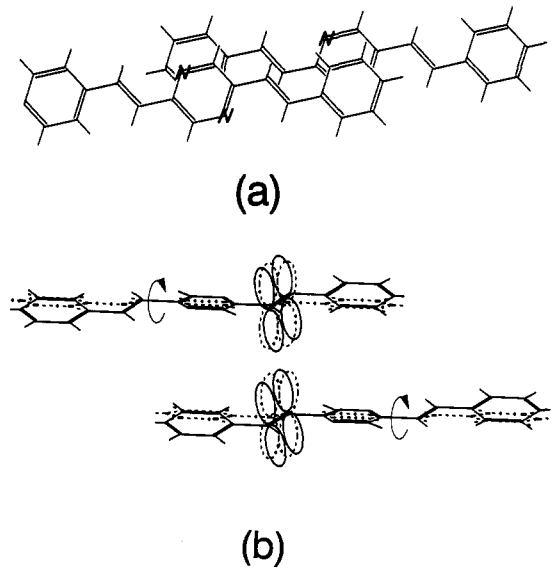

Figure 6. (a) Projection of reacting molecules showing their lateral displacement. (b) Side view of reacting molecules showing librational motion about the x-axis associated with modes most involved in the reaction. The π orbitals associated with the ethylenic centers forming the cyclobutyl ring of the oligomer are also depicted.

the dynamical matrix in the harmonic approximation. From this, lattice vibrational frequencies and associated eigenvectors are obtained. The latter describe the motions of the molecules and symmetry for each vibrational mode. The experimental lattice parameters of a = 20.638 Å, b = 9.599 Å, and c = 7.655 Å[8] compared favorably to those obtained after minimization by the calculation of a = 20.780 Å, b = 10.464 Å, and c = 7.140 Å. In this regard, it should be remembered that the calculations are for the equilibrium lattice at 0 K. The calculated mode symmetries agreed with those observed experimentally for all the Raman active modes while the frequencies varied by less than 5 cm^{-1} on average (Table IV). Such good agreement between the experimental and calculated frequencies and symmetries indicates that the calculational method acceptably models the lattice potential.

Of importance to the consistency of the topochemical postulate and the proposed phonon-assistance mechanism is the motion associated with the 84.25-cm^{-1} B_{2g} mode since it is so markedly affected by the reaction. By using the axial assignments in Figure 1a, the normalized, axial, displacement vectors for the 84.25-cm^{-1} B_{2g} mode describe essentially rotational vibrations about the molecular x-axis. The calculations indicate similar molecular motions for the 67.25-cm^{-1} A_g and the 136.75-cm^{-1} B_{1g} modes.

IV. Discussion

To assess the contributions these phonons make to the progress of the reaction, it is necessary to consider more closely the geometry of the reacting monomers. Figure 6a shows a reactive monomer pair projected onto the plane of the pyrazine ring of one of the molecules in order to show that the reactive double bonds are laterally displaced from one another by a small distance. For facile reaction of the ethylenic π-orbitals, it is necessary that the reacting molecules be brought into a position that will allow favorable orbital overlap essential to form product. As shown by the lattice dynamical calculations, the motion associated with the 84.25-cm^{-1} B_{2g} mode is largely a rotation about the x-axis. Since a monomer can only react with its counterpart in an adjacent unit cell and the collective nature of the vibrations requires in-phase motions, both molecules must be rotating in the same direction at the same time. This motion will bring the necessary orbitals into a more favorable position to react since the concerted rotations compensate for the lateral displacement as shown in Figure 6b. Because the major components of motion of the other

two modes identified above are similar to those of the 84.25-cm^{-1} mode, the same argument obtains for them as well. These librational motions can effectively aid in the interactions necessary for reaction; they are in accord with a phonon-assistance mechanism. This scenario rationalizes why these particular modes are most affected by the reaction.

Consistency of the topochemical postulate with the above results requires that the calculated vibrations should correspond to the least motion for the reaction to occur. The motion associated with these modes must bring the ethylenic π-orbitals into a correct orientation for the cyclization reaction. A possibility would be motion of both molecules about the z-axis, but this would require extreme movements of the distal phenyl rings which would be far from the path of least motion. However, rotations consistent with the modes identified by Raman spectroscopy in this study and with motions calculated by lattice dynamical calculations (Figure 6b) are well in agreement with the requirements of the topochemical postulate. These motions merely involve quasirotations of each monomer about its long axis and would be the least movement required for reaction.

The monomer rotation is consistent with the crystallographic results because it requires the carbon atoms of the ethylenic double bonds to move toward each other to form the cyclobutane ring. Initially, these carbons are 3.94 Å apart, which is larger than twice the typical single carbon–carbon bond distance of 1.54 Å. On the basis of the results from the refinement in which the oligomer was treated as a rigid body, the two independent C atoms move an average of 1.11 Å; the average displacement for both a pyrazine non-hydrogen atom and a phenyl C atom is 0.41 Å. Framework (DSP) and ball and stick (oligomer) depictions are superimposed on the electron density in Figure 5 to provide an impression of the changes in atomic positions on going from the monomer to the oligomer. The monomers selected for this illustration in Figure 5 correspond to those shaded for emphasis in the packing diagram (Figure 4).

Mode softening could be more a *result* of the photoreaction rather than necessarily being associated *with* the reaction itself. Indeed, this argument may be posed in general for phonon assistance. Further experiments on additional systems will be necessary to completely elucidate the validity of this mechanism. However, the present results are entirely consistent with phonon assistance.

The observation that the crystal structure model refined much better when minimizing ΔF^2 than ΔF provides evidence that the crystal is heterogeneous, that is, it consists of domains of monomers and oligomers rather than a homogeneous distribution of these components. This heterogeneity is on the scale of the X-ray wavelength. However, on the 1000-fold larger scale of the wavelength of the Raman experiment, the crystal reaction is homogeneous.

Studies such as this place quantitative limits on the qualitative statements of "small displacements" described by the topochemical postulate. The 1.11-Å motion is on the order of a bond length (C–H) and delineates the range of motion for this typical topochemical reaction. The distance obviously relates to the commonly accepted limiting average intermolecular spacing of 4.0 Å. Not surprisingly, the largest motions are associated with those atoms involved in forming the new bonds.

V. Conclusions

This research provides a more detailed quantitative foundation for postulates fundamental to the understanding of solid-state reactions by direct examination of the lattice energetics, dynamics, and structure for a partially reacted crystal. Individually, these studies cannot yield the comprehensive information required to describe and predict reactivity of molecular crystals. By examination of a partially reacted crystal, a "snapshot" giving information on the dynamics and structural evolution of the reaction can be obtained. A sequence of such studies on crystals with differing extents of reaction can provide the most detailed picture yet possible of a solid-state reaction. The topochemical postulate concerns packing geometry, which is a consequence of the lattice potential that is directly probed by phonon spectroscopy and lattice dynamics. X-ray crystallography, lattice spectroscopy, and lattice dynamics are necessary complements to each other to fully elucidate solid-state reactions. The results of this work describe an effective approach to the direct investigation of the topochemical postulate and the mechanism of phonon assistance. It is likely that to advance our detailed understanding of these concepts additional studies which employ concerted structural, dynamical, and theoretical aspects in the study of organic solid-state reactions will have to become the norm rather than the exception. Indeed, upon further investigation it may be found that these postulates are only zeroth-order approximations of more universal and fundamental principles.

Acknowledgment. N.M.P. thanks the University of Nebraska and the University of Nebraska Foundation for support through graduate fellowships; P.G. thanks the Center for Biotechnology of the University of Nebraska for a graduate fellowship. We thank S. Henkel of the Institute für Organische Chemie der Universität Stuttgart for measuring the single-crystal X-ray diffraction data.

Supplementary Material Available: Table of atomic anisotropic displacement parameters (1 page); listing of structure factors (12 pages). Ordering information is given on any current masthead page.